ISSN 1063-7788, Physics of Atomic Nuclei, 2019, Vol. 82, No. 2, pp. 134–143. © Pleiades Publishing, Ltd., 2019.
Russian Text © V.A. Okorokov, 2019, published in Yadernaya Fizika, 2019, Vol. 82, No. 2, pp. 147–157.

ELEMENTARY PARTICLES AND FIELDS
Experiment

Energy Dependence of the Ratio of the Elastic-to-Total Cross Sections for Proton–Proton and Antiproton–Proton Collisions

V. A. Okorokov*

National Research Nuclear University MEPhI, Moscow, 115409 Russia

Received July 26, 2018; revised July 26, 2018; accepted July 26, 2018

Abstract—The results obtained from a phenomenological analysis of the ratio of the elastic-to-total cross sections for proton–proton (pp) and antiproton–proton ($\bar{p}p$) scattering as a function of energy are presented. Analytic functions proposed on the basis of studying low- and high-energy experimental data for various scattering parameters make it possible to obtain a statistically acceptable quantitative description of the energy dependence of this ratio over a broad energy region of $\sqrt{s} \geq 3$ GeV for individual samples of pp and $\bar{p}p$ collisions and over the region of $\sqrt{s} \geq 5$ GeV for a combined ensemble of experimental data. On the basis of the resulting approximations, the ratio of the elastic-to-total cross sections for pp collisions are estimated at various values of $\sqrt{s}$ up to an ultrahigh energy of $\sqrt{s} = 10$ PeV. The resulting estimates may prove to be useful for experiments at currently operating and future hadron colliders, as well as for measurements of ultrahigh-energy cosmic rays. An indication of the onset of the asymptotic region for the cross-section ratio in question is observed in the region of $\sqrt{s} \gtrsim 5$–10 PeV.

DOI: 10.1134/S1063778819010113

INTRODUCTION

Experimental data indicate unambiguously that, in proton–proton (pp) and antiproton–proton ($\bar{p}p$) interactions, the elastic cross section ($\sigma_{\rm el}$) grows faster with collision energy ($\sqrt{s}$) than the total cross section ($\sigma_{\rm tot}$). As a result, that the survival probability for a beam of (anti)nucleons grows with s; this experimental fact is of importance and is somewhat unexpected. It should be emphasized that the nature of this effect has yet to be clarified conclusively; moreover, an enhanced growth of $\sigma_{\rm el}(s)$ with respect to $\sigma_{\rm tot}(s)$ has been studied less vigorously than the energy dependence of the total cross section for pp and $\bar{p}p$ collisions. The possible interplay between the behavior of $\sigma_{\rm el}$ as a function of energy and, hence, the behavior of the survival probability in (anti)nucleon collisions, on one hand, and Bose–Einstein condensation and the topology of the QCD vacuum, on the other hand, was examined in [1]. As was discussed in [2], the structure of the QCD vacuum may be characterized by highly irregular fractal-like geometry. Moreover, one can assume that the interaction region may have a complicated geometric shape corresponding to fractal geometry rather than to the simplest cases of Euclidean geometry. This entails the assumption that both the topological properties of the QCD vacuum and the type of geometry used to approximate the shape of colliding particles exert influence on the s dependence of global parameters, especially cross sections for hadron scattering. In general, this assumption implies a fundamental interplay between geometry and dynamics of strong-interaction processes. However, these qualitative arguments should be tested via a quantitative analysis of experimental data.

It is also important to study the asymptotic behavior of global parameters of hadron scattering—in particular, pp and $\bar{p}p$ scattering—and to address the problem of searches for the onset of the asymptotic region in the collision energy. The asymptotic relations in question are based on fundamental properties of quantum field theory—namely, the analyticity of the scattering amplitude and the unitarity condition. Further, processes in which the momentum transfer is low make a dominant contribution to the cross section for hadron interactions at high s. In view of this, phenomenological investigations into the behavior of the respective cross sections and their ratios versus s open wide possibilities for analyzing QCD-based models—in particular, the approach of a gluon (or glueball) cloud at long distances.

Thus, study of the ratio of the cross sections $\sigma_{\rm tot}$ and $\sigma_{\rm el}$ in hadron interactions as a function of the collision energy is of importance both for the development of strong-interaction theory—in particular, theory of the soft-physics sector—and, in a more general case, for analysis of the fundamentals of quantum field theory.

*E-mail: VAOkorokov@mephi.ru;Okorokov@bnl.gov

1. OBSERVABLES AND APPROXIMATING FUNCTIONS

In the present study, the ratio of the elastic-to-total cross sections,

$$R_{\text{el/tot}} = \sigma_{\text{el}}/\sigma_{\text{tot}}, \tag{1}$$

is studied as a function of the collision energy in pp and $\bar{p}p$ interactions. For pp scattering, the experimental data sample used for the set $\mathcal{G}_{pp} \equiv \{\mathcal{G}_{pp}^i\}_{i=1}^2 = \{\sigma_{\text{tot}}^{pp}, \sigma_{\text{el}}^{pp}\}$ of global scattering parameters was formed by employing the database in [3], while, for $\bar{p}p$ scattering, the data for the analogous set $\mathcal{G}_{\bar{p}p}$ were taken from [4]. For the experimental points, we set the total errors to the values calculated as $\Delta_{\text{tot}}^2 = \Delta_{\text{stat}}^2 + \Delta_{\text{syst}}^2$, where Δ_{stat} and Δ_{syst} are, respectively, statistical and systematic errors [5].

The dependences $\sigma_{\text{tot}}(s)$ and $\sigma_{\text{el}}(s)$ exhibit similar basic features and functional behavior over a broad energy range. In general, σ_{tot} for pp and $\bar{p}p$ collisions behave qualitatively at high energies as $\ln^{\alpha}\varepsilon$, where $0 < \alpha \leq 2$, $\varepsilon \equiv s/s_0$, and $s_0 = 1$ GeV^2. This dependence arises in various approaches [3–5]. On the other hand, a term proportional to $\varepsilon^{-\beta}$, which was proposed within axiomatic quantum field theory (AQFT) [6], makes it possible to describe reasonably experimental data at low energies down to $\sqrt{s} = 3$ GeV [4, 6]. Additionally, a detailed analysis of the energy dependence of the diffraction-cone slope B in elastic scattering shows that, in constructing approximations in the region of low and intermediate values of the collision energy s, a function proportional to $\ln^{-\gamma}\varepsilon$ leads to χ^2 values per degree of freedom that are close to those that are obtained in the case of employing a power-law term [7]. Therefore, either of the two functions under discission can be viewed as a possible approximation for the low-energy behavior of the parameters from the set $\mathcal{G}_{pp/\bar{p}p}$. With allowance for the above arguments and for the form of the experimental dependences of the ratio in (1) on s in various collisions (see below), analytic approximations of $R_{\text{el/tot}}(s)$ are taken here in the form

$$R_{\text{el/tot}}(s) = a_1 + a_2 \ln^{a_3}\varepsilon + a_4 \ln^{-a_5}\varepsilon \tag{2a}$$

or in the form

$$R_{\text{el/tot}}(s) = a_1 + a_2 \ln^{a_3}\varepsilon + a_4 \varepsilon^{-a_5}, \tag{2b}$$

where the values of the free parameters a_i, $i = 1$–5, depend on the fitting range—that is, on the lower boundary of the energy interval $s \geq s_{\text{min}}$. We assume that the second terms in Eqs. (2) describe the high-energy behavior of $R_{\text{el/tot}}(s)$, while the third terms describe the region of low and intermediate energies.

In [8], it was shown that the upper bound on the inelastic cross section (σ_{inel}) for hadron interaction at high energy is $1/4$ of the respective upper bound on σ_{tot}; that is, we have $\left[\sup\sigma_{\text{inel}}(s)/\sup\sigma_{\text{tot}}(s)\right]_{s\in\mathbf{S}_h\subset\mathbf{S}} = 1/4$ in the high-energy subinterval $\mathbf{S}_h \subset \mathbf{S}$, assuming identical regions in energy, $\mathbf{S} \equiv (4m_p^2, \infty)$, for all of the cross sections being considered (σ_{tot}, σ_{el}, and σ_{inel}), where m_p is the proton mass [5] and the lower bound on $\mathbf{S}$, $s_{\text{l.b.}} \equiv 4m_p^2$, corresponds to the interactions being discussed (pp and $\bar{p}p$). On the basis of general assumptions on the properties of the scattering amplitude for $\varkappa_1 + \varkappa_2 \to \varkappa_3 + \varkappa_4$ binary processes, it can be shown that, within AQFT, the cross sections $\sigma_{\text{tot}}(s)$ and $\sigma_{\text{el}}(s)$ are locally integrable functions for $s \in \mathbf{S}$ [9]. This means that these functions possess the property of Riemann integrability for $\forall[s_1, s_2] \subset \mathbf{S}$. By virtue of the necessary condition for Riemann integrability, the cross sections $\sigma_{\text{tot}}(s)$ and $\sigma_{\text{el}}(s)$ are bounded functions for $\forall[s_1, s_2] \subset \mathbf{S}$ (see, for example, [10]). Because of the unitarity condition $\sigma_{\text{tot}} = \sigma_{\text{el}} + \sigma_{\text{inel}}$ and the linearity properties, $\sigma_{\text{inel}}(s)$ also possesses all of the aforementioned properties. At the present time, a commonly prevalent opinion is that it is reliably established—both theoretically and experimentally—that all of the cross sections being considered grow with s, at least at high energies [5]. Therefore, the following statements are valid: (i) $\forall i$ (i = tot, inel, el), $\exists \lim_{s\to\infty}\sigma_i(s) \equiv L_i$ and L_i is finite; (ii) $\forall i$ (i = tot, inel, el), $\sup_{s\in\mathbf{S}_h}\sigma_i(s) = \lim_{s\to\infty}\sigma_i(s)$. We then have

$$\frac{\sup_{s\in\mathbf{S}_h\subset\mathbf{S}}\sigma_{\text{inel}}(s)}{\sup_{s\in\mathbf{S}_h\subset\mathbf{S}}\sigma_{\text{tot}}(s)} = \frac{\lim_{s\to\infty}\sigma_{\text{inel}}(s)}{\lim_{s\to\infty}\sigma_{\text{tot}}(s)} \tag{3}$$

$$= \lim_{s\to\infty}\frac{\sigma_{\text{inel}}(s)}{\sigma_{\text{tot}}(s)} \equiv \lim_{s\to\infty} R_{\text{inel/tot}}(s),$$

where $R_{\text{inel/tot}} = \sigma_{\text{inel}}/\sigma_{\text{tot}}$. With allowance for the unitarity condition, this means that

$$[R_{\text{el/tot}}(s)]_{s\to\infty} \to 3/4. \tag{4}$$

The two approximating functions in (2) exhibit the same asymptotic behavior,

$$[R_{\text{el/tot}}(s)]_{s\to\infty} \approx a_1 + a_2 \ln^{a_3}\varepsilon, \tag{5}$$

since, for $s \to \infty$, the contributions of the terms corresponding to the low-energy region in expressions (2a) and (2b) become negligible. As a consequence, we obtain the relation

$$s_{\text{a}} \sim s_0 \exp\left\{[(3/4 - a_1)/a_2]^{1/a3}\right\} \tag{6}$$

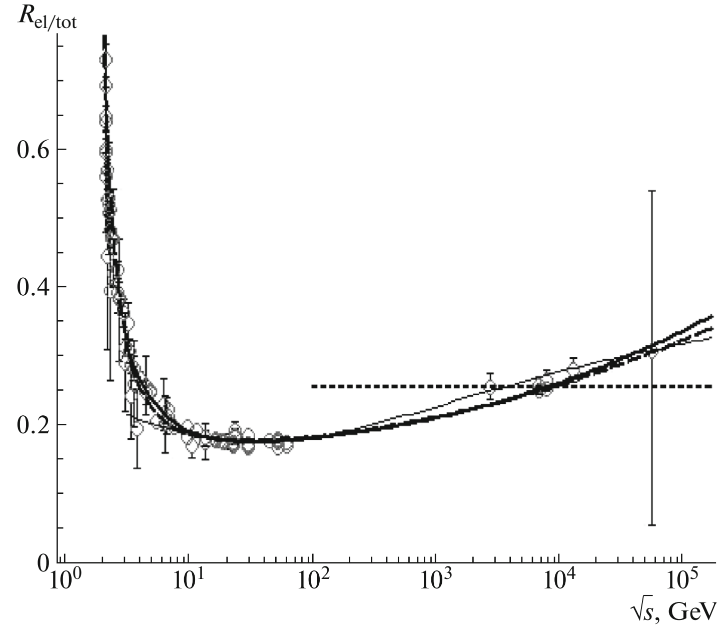

Fig. 1. Energy dependence of the ratio of σ_{el} to σ_{tot} in pp collisions: (dashed curve) approximation by the function in Eq. (2a) at $\sqrt{s_{min}} = 2$ GeV, (thick solid curve) approximation by the function in Eq. (2b) at $\sqrt{s_{min}} = 3$ GeV, (dotted curve) approximation by a constant at $\sqrt{s_{min}} = 100$ GeV (for a detailed description, see the main body of the text), (thin solid curve) ratio of the approximation of $\sigma_{el}(s)$ from [12] to the approximation of $\sigma_{tot}(s)$ from [5], and (points) experimental data from [3].

for the collision energy at which one expects the onset of the asymptotic regime in pp and $\bar{p}p$ interactions.[1)]

The experimental feature in (1) may also be related to the parameter $\kappa(s) \equiv \sigma_{tot}(s)/8\pi B(s)$, which is treated as a signature of the onset of the asymptotic region for global scattering parameters such as $\sigma_{tot}(s)$ and $B(s)$ [3], by the equations

$$\kappa(s) = 2R_{el/tot}(s)\left[1 + \rho^2(s)\right]^{-1}, \qquad (7)$$
$$\lim_{\rho \to 0} \kappa(s) = 2R_{el/tot}(s),$$

where $\rho(s) \equiv \mathrm{Re}F(s,0)/\mathrm{Im}F(s,0)$ is the ratio of the real-to-imaginary parts of the forward-scattering amplitude. It is noteworthy that, in accordance with experimental data, $|\rho(s)| \lesssim 0.3(0.2)$ for $\sqrt{s} \gtrsim 5(3)$ GeV in pp ($\bar{p}p$) collisions [4]. Therefore, the limiting transition in Eq. (7) is valid over a broad range of energies both in pp and $\bar{p}p$ scattering at a precision level better than 0.1.

[1)]Obviously, the estimated lower boundary of the asymptotic region, s_a, is a physically objective quantitative feature that is constant, at least for the observable being considered—in particular, it is independent of a specific form of the approximating function for this observable. The form of this function is determined exclusively by the respective relation between the estimated asymptotic energy and the fitted values of the adjustable parameters.

2. EXPERIMENTAL DATA AND RESULTS OF FITTING

Figures 1 and 2 show the ratio in (1) as a function of $\sqrt{s}$ for respectively, pp and $\bar{p}p$ collisions [11]. Experimental data for $R_{el/tot}$ are available in the region of $\sqrt{s} \geq 2.03$ (1.89) GeV for elastic pp ($\bar{p}p$) scattering. The presence of a sharp peak in $R_{el/tot}(s)$ near the lower boundary $\sqrt{s_{l.b.}}$ for $\bar{p}p$ scattering (see Fig. 2) a priori prevents the use of Eqs. (2) in approximating all available data. Therefore, the lowest value of $\sqrt{s}$ at which the dependence $R_{el/tot}(s)$ can be approximated by the functions in (2) both for pp and $\bar{p}p$ collisions should not be less than 2 GeV. Moreover, the experimental data for $R_{el/tot}$ in Fig. 1 agree qualitatively with a constant in the region of $\sqrt{s} \geq 100$ GeV; possibly, this statement is also valid for $\bar{p}p$ collisions, but the number of experimental points is small here (see Fig. 2). Therefore, the dependence $R_{el/tot}(s)$ is additionally approximated by a constant, $R_{el/tot}(s) = a_0$, at $\sqrt{s_{min}} = 100$ GeV for reactions induced by elastic pp and $\bar{p}p$ scattering.[2)] The fitted values of the

[2)]From Figs. 1 and 2, one can see that there is a large gap between measurements at the highest energy of the ISR (Intersecting Storage Rings) accelerator, $\sqrt{s} \approx 63$ GeV, and the closest right point at $\sqrt{s} = 2760$ (546) GeV for pp ($\bar{p}p$) interactions. Therefore, the value of $\sqrt{s} = 100$ GeV was chosen by convention for the interval where a constant was taken to be an approximant; this value is used below without any loss of generality.

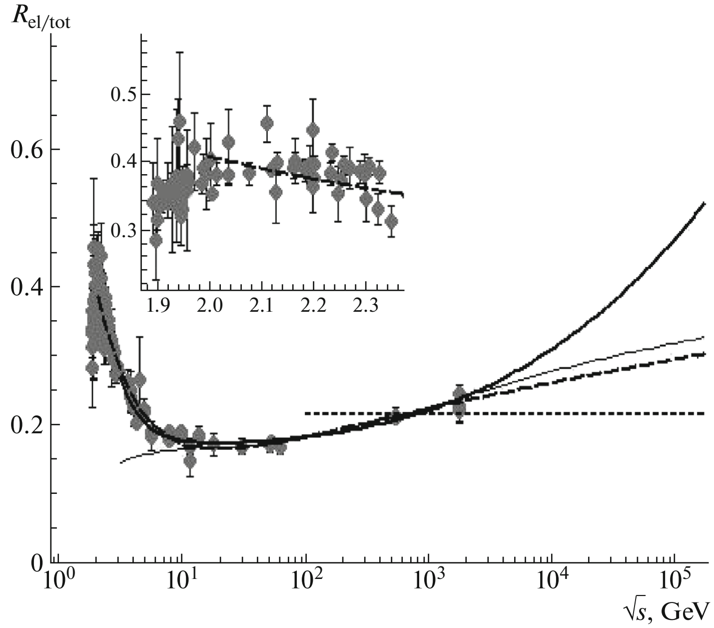

Fig. 2. Ratio of σ_{el} to σ_{tot} as a function of $\sqrt{s}$ for $\bar{p}p$ collisions: (dashed curve) approximation by the function in Eq. (2b) at $\sqrt{s_{\min}} = 2$ GeV, (thick solid curve) approximation by the function in Eq. (2b) at $\sqrt{s_{\min}} = 3$ GeV, (dotted curve) approximation by a constant at $\sqrt{s_{\min}} = 100$ GeV (for a detailed description, see the main body of the text), (thin solid curve) ratio of the approximation of $\sigma_{\mathrm{el}}(s)$ from [12] to the analytic function describing $\sigma_{\mathrm{tot}}(s)$ in [5] and (points) experimental data from [4]. The inset shows experimental data and an approximating curve for the narrow interval of $\sqrt{s} = 1.86-2.36$ GeV near the lower boundary in energy.

adjustable parameters in the approximations of the experimental dependences $R_{\mathrm{el/tot}}(s)$ by the proposed functions are given in Tables 1 and 2 at various values of $s_{\min}$ for, respectively, pp and $\bar{p}p$ collisions.

At $\sqrt{s_{\min}} = 2$ GeV, the quality of the fit proves to be low for both of the approximations in (2) for elastic pp interactions, even though the function in (2a) leads to a substantially better value of χ^2/NDF than the function in (2b) does; in the case of $\bar{p}p$ scattering, the relationship between the χ^2/NDF values for the functions in (2a) and (2b) is opposite. From Tables 1 and 2, one can see that either of the two functions in (2) provides an approximation of a statistically acceptable quality for the experimental dependence $R_{\mathrm{el/tot}}(s)$ in pp and $\bar{p}p$ collisions over a wide region of $\sqrt{s} \geq 3$ GeV, which covers the energy region where the approximation $1 + \rho^2 \approx 1$ is valid at a precision level not poorer than 0.09 and 0.04, respectively. Therefore, the discussion in the remaining part of this paragraph is concentrated on the results for values in the region of $\sqrt{s_{\min}} \geq 3$ GeV (see Tables 1 and 2). For pp collisions, the behavior of the generalized logarithmic function in Eq. (2a) at high energies is close to $\ln \varepsilon$, especially at $\sqrt{s_{\min}} = 3$ GeV; at the same time, the function in Eq. (2b) leads to a substantially faster growth in the region of high energies at the respective value of $s_{\min}$—namely, the value of a_3 complies with 2.0 within two standard deviations. In the case of $\bar{p}p$ interactions, the fitted values of the parameter a_3 exhibit a large spread (see Table 2): the function in Eq. (2a) is close to $\ln \varepsilon$ at high energies for $\sqrt{s_{\min}} = 3$ GeV, whereas the value of a_3 agrees with 2.0 within two standard deviations at larger values of $s_{\min}$; the function in Eq. (2b) leads to a large difference between the approximating curves at different values of $s_{\min}$ at high energies—in particular, the fitted result obtained on the basis of the function in Eq. (2b) at $\sqrt{s_{\min}} = 3$ GeV exhibits a very fast growth. Although the functions in Eqs. (2a) and (2b) lead to close values of χ^2/NDF, the behavior of $R_{\mathrm{el/tot}}(s)$ for low and intermediate values of s is described somewhat better by a power-law dependence on ε than by a power of $\ln \varepsilon$. At $\sqrt{s_{\min}} = 100$ GeV, a constant complies with the experimental points for both collision types (pp and $\bar{p}p$) at a quantitative level.

A comparison of the approximating curves obtained for the different functions in Eqs. (2) and different values of $s_{\min}$ makes it possible to draw the following conclusions. According to numerical results obtained upon applying the fitting procedure (see Tables 1 and 2), the dependence on the approximating-function type at a fixed value in the range of $\sqrt{s_{\min}} = 2-5$ GeV manifests itself most strongly at the smallest of the values considered here for the lower boundary of the fitting interval

Table 1. Fitted values of the parameters in $R_{\mathrm{el/tot}}(s)$ for elastic pp scattering

$\sqrt{s_{\min}}$, GeV	Parameter					
	a_1	$a_2 \times 10^3$	a_3	a_4	a_5	χ^2/NDF
			(2a)			
2	0.1596 ± 0.0015	0.136 ± 0.016	2.26 ± 0.04	1.57 ± 0.04	2.71 ± 0.05	371/87
3	0.016 ± 0.009	15 ± 4	0.94 ± 0.08	0.74 ± 0.06	1.20 ± 0.10	55.5/55
5	0.052 ± 0.025	3.8 ± 1.6	1.33 ± 0.11	0.481 ± 0.019	0.95 ± 0.08	41.9/41
			(2b)			
2	0.1794 ± 0.0008	$(7.4 \pm 2.0) \times 10^{-5}$	4.79 ± 0.09	3.91 ± 0.27	1.40 ± 0.04	516/87
3	0.164 ± 0.003	0.06 ± 0.04	2.55 ± 0.25	0.87 ± 0.14	0.76 ± 0.06	54.5/55
5	0.157 ± 0.005	0.16 ± 0.09	2.23 ± 0.19	0.44 ± 0.17	0.58 ± 0.11	41.6/41
			constant			
10^2	0.255 ± 0.004	–	–	–	–	3.04/6

Table 2. Fitted values of the parameters in $R_{\mathrm{el/tot}}(s)$ for elastic $\bar{p}p$ scattering

$\sqrt{s_{\min}}$, GeV	Parameter					
	a_1	$a_2 \times 10^3$	a_3	a_4	a_5	χ^2/NDF
			(2a)			
2	$(2.50 \pm 0.04) \times 10^{-4}$	3.2 ± 1.2	1.52 ± 0.13	0.542 ± 0.007	0.86 ± 0.03	334/88
3	0.089 ± 0.017	8 ± 4	1.03 ± 0.13	0.69 ± 0.06	1.76 ± 0.09	32.3/28
5	0.137 ± 0.016	0.17 ± 0.09	2.33 ± 0.20	0.24 ± 0.08	1.2 ± 0.4	12.2/16
			(2b)			
2	0.025 ± 0.008	41 ± 6	0.60 ± 0.07	0.776 ± 0.024	0.61 ± 0.03	266/88
3	0.170 ± 0.005	0.0066 ± 0.0026	3.4 ± 0.8	1.5 ± 0.8	1.17 ± 0.22	31.6/28
5	0.058 ± 0.027	5 ± 3	1.331 ± 0.024	0.21 ± 0.06	0.19 ± 0.13	11.8/16
			constant			
10^2	0.217 ± 0.005	–	–	–	–	7.03/4

in s and becomes weaker with increasing $s_{\min}$ both for pp and for $\bar{p}p$ collisions. At $\sqrt{s_{\min}} = 2$ GeV, a sizable distinction is observed between the curves obtained with the aid of the functions in Eqs. (2a) and (2b) for $\sqrt{s} \gtrsim 100$ GeV for pp collisions and even for $\sqrt{s} \gtrsim 20$ GeV for $\bar{p}p$ collisions. The range within which the results based of the approximations by the the functions in Eqs. (2a) and (2b) behave similarly becomes substantially broader at larger values of $s_{\min}$. The respective curves prove to be close to each other in the region of $\sqrt{s} \gtrsim 10$ (1) TeV at $\sqrt{s_{\min}} = 3$ GeV and in the region of $\sqrt{s} \gtrsim 100$ (10) TeV at $\sqrt{s_{\min}} = 5$ GeV for pp ($\bar{p}p$) scattering; that is, the approximating curves for pp or $\bar{p}p$ data depend only slightly in the last case on the type of the functions in Eqs. (2) at any energies reached experimentally. The situation around the dependence of the approximating curves on $s_{\min}$ for a fixed type of the functions in Eqs. (2) is similar for the elastic-collision types being studied. In the energy range measured experimentally, the curves obtained on the basis of the function in Eq. (2a) behave similarly for all of the $s_{\min}$ values being considered, especially at $\sqrt{s_{\min}} = 3$ and 5 GeV, the difference between the approximations being somewhat greater for $\bar{p}p$ than for pp interactions. For the function in Eq. (2b), the approximating curve for $\sqrt{s_{\min}} = 2$ GeV differs substantially from the other two, which are nearly coincident in the region of $5 \leq \sqrt{s} < 10^5$ (2000) GeV for pp ($\bar{p}p$) collisions. The qualitative relations indicated above for various approximating curves are generated primarily by the effect of low-energy data, which are removed from approximated data samples for $\sqrt{s_{\rm min}} \geq 3$ GeV.

The smooth curves in Figs. 1 and 2 correspond to the best fitted results at $\sqrt{s_{\rm min}} = 2$ and 3 GeV; that is, the approximation by the function in Eq. (2a) and the approximation by the function in Eq. (2b) for pp collisions are shown in accordance with Table 1 at, respectively, $\sqrt{s_{\rm min}} = 2$ GeV and $\sqrt{s_{\rm min}} = 3$ GeV. According to Table 2, the curves obtained on the basis of the function in Eq. (2b) at either of the above two values of $\sqrt{s_{\rm min}}$ correspond to the elastic $\bar{p}p$ reaction. The functions proposed in Eqs. (2a) and (2b) are in reasonable agreement with experimental data up to $\sqrt{s_{\rm min}} = 2$ GeV both for pp (Fig. 1) and for $\bar{p}p$ scattering (Fig. 2). The approximating curves in Fig. 1 for pp collisions behave similarly at all energies accessible experimentally, whereas the approximation for $\bar{p}p$ collisions at $\sqrt{s_{\rm min}} = 2$ GeV grows substantially slower in the high-energy region than its counterpart constructed at $\sqrt{s_{\rm min}} = 3$ GeV (see Fig. 2). The inset in Fig. 2 shows in detail the change in the trend exhibited by $R_{\rm el/tot}(s)$ near the lower threshold energy $\sqrt{s_{\rm l.b.}}$ for $\bar{p}p$ collisions and confirms the validity of the approximations of available experimental data by the functions in (2) in the region of $\sqrt{s} \geq 2$ GeV. As was indicated above, the approximating curve constructed on the basis of the function in Eq. (2b) at $\sqrt{s_{\rm min}} = 3$ GeV for $\bar{p}p$ collisions exhibits a very fast growth in the region of multi-TeV energies in relation to the other approximations for $\bar{p}p$ collisions and in relation to the respective curve for pp collisions. However, this distinction may be due to the absence of experimental points for the first case in the region of $\sqrt{s} > 2$ TeV. In order to draw more reliable physical conclusions on the high-energy behavior of $R_{\rm el/tot}(s)$ in Fig. 2, it is therefore highly desirable to have new experimental data for $\bar{p}p$ collisions at multi-TeV energies. The results of the present study are compared with the ratio of the function approximating $\sigma_{\rm el}$ in [12] to “standard” smooth approximations of $\sigma_{\rm tot}$ for pp and $\bar{p}p$ reactions from [5] (thin solid lines in Figs. 1 and 2, respectively). As might have been expected, these curves lie somewhat lower than the majority of the experimental points for $\sqrt{s} < 10$ GeV, since the approximation in question was constructed for $\sigma_{\rm el}$ only in the region of $\sqrt{s} \geq 10$ GeV [12]. For pp collisions, there is a sizable discrepancy between the smooth curves based on expressions (2) and the approximation based on the parametrizations from [5, 12] in the energy range of $\sqrt{s} \sim 0.3$–30 TeV (Fig. 1). New experimental data would be of use in choosing a preferable approach. Such data could be obtained at the Relativistic Heavy Ion Collider (RHIC) in the range of $\sqrt{s} \sim 0.1$–0.5 TeV and in the low-energy mode at the Large Hadron Collider (LHC) at $\sqrt{s} \sim 1.0$ TeV. The curve obtained for pp collisions on the basis of the results from [5, 12] exhibits a slower growth for $R_{\rm el/tot}(s)$ in the ultrahigh-energy region of $\sqrt{s} \gtrsim 100$ TeV in relation to the functions in (2) at various values of $s_{\rm min}$, and this feature may prove to be of importance for assessing the onset of the asymptotic regime. The approximating curve calculated for $\bar{p}p$ collisions on the basis of the parametrizations from [5, 12] is very close to the curves characterized by the best values of χ^2/NDF and obtained in the present study at $\sqrt{s_{\rm min}} = 2$ and 3 GeV in the energy range of $10 \lesssim \sqrt{s} \lesssim 2000$ GeV, but some discrepancy appears at higher energies (see Fig. 2). This difference between the different approximations of $R_{\rm el/tot}(s)$ for $\bar{p}p$ collisions grows with s.

Figures 1 and 2 show that the experimental dependences $R_{\rm el/tot}(s)$ for pp and $\bar{p}p$ collisions behave similarly, at least at a qualitative level, in the region $\sqrt{s} > 2$ GeV—that is, over the whole region of $\sqrt{s}$ where a comparison is possible. For this reason, the ratio in (1) was also analyzed for a combined data sample that includes data for pp and $\bar{p}p$ interactions.[3)] Figure 3 gives the experimental dependence $R_{\rm el/tot}(s)$ for nucleon–nucleon scattering along with the approximations described in detail below. The fitted values of adjustable parameters in the approximation of $R_{\rm el/tot}(s)$ by the functions in Eqs. (2) are presented in Table 3 for various values of $\sqrt{s_{\rm min}}$. At any value in the range of $\sqrt{s_{\rm min}} = 2$–5 GeV, the χ^2/NDF values characterizing the description of the data sample for the ratio in (1) for nucleon–nucleon scattering in terms of the functions in Eqs. (2a) and (2b) are close to each other, but only at $\sqrt{s_{\rm min}} = 5$ GeV is the quality of this description statistically acceptable. Moreover, the function in Eq. (2b) provides a somewhat better fit, especially at $\sqrt{s_{\rm min}} = 2$ GeV, than the generalized logarithmic function in Eq. (2a). In contrast to the case of approximations of individual data sets for pp and $\bar{p}p$ collisions, an approximation of the ratio $R_{\rm el/tot}(s)$ for the combined set of data on nucleon–nucleon collisions by a constant with a statistically acceptable quality is possible only in the TeV-energy range. Since experiments on pp scattering make a dominant contribution in this region of s,

[3)] For the sake of brevity, the combined data sample is also referred to below as a data sample for nucleon–nucleon scattering.

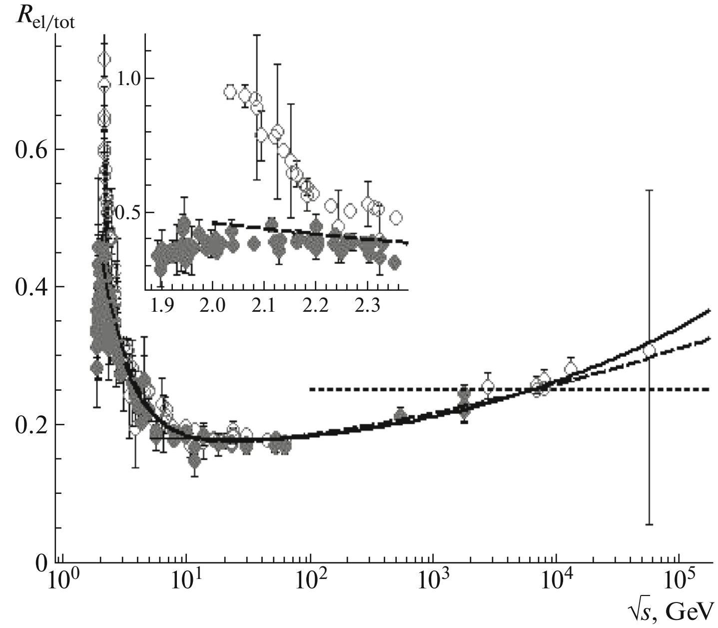

Fig. 3. Ratio $R_{\text{el/tot}}$ as a function of $\sqrt{s}$ for a combined sample of data on (open symbols) pp and (closed symbols) $\bar{p}p$ collisions: (dashed curve) approximation by the function in Eq. (2b) at $\sqrt{s_{\min}} = 2$ GeV, (thick solid curve) approximation by the function in Eq. (2b) at $\sqrt{s_{\min}} = 3$ GeV, (dotted curve) approximation by a constant at $\sqrt{s_{\min}} = 1$ TeV, (thin solid curve) approximation by a constant in the intermediate-energy range at $\sqrt{s_1} = 10$ GeV (for a detailed description, see the main body of the text), and (points) experimental data from [3, 4]. The inset shows experimental data and an approximating curve for the narrow interval of $\sqrt{s} = 1.86{-}2.36$ GeV near the lower boundary in energy.

the value of the constant a_0 for the combined data sample agrees, as might have been expected, within the errors with its value for pp interactions. The inset in Fig. 3 shows in detail the behavior of $R_{\text{el/tot}}(s)$ near the lower boundary $\sqrt{s_{\text{l.b.}}}$ for pp and $\bar{p}p$ interactions. In this interval of s, the experimental points for pp and $\bar{p}p$ interactions exhibit a large spread, which leads to an unacceptably large value of χ^2/NDF at $\sqrt{s_{\min}} =$ 2 GeV. On the other hand, the experimental results for collisions of the type being considered show similar trends—specifically, a decrease in the ratio in (1) as the collision energy grows—for $\sqrt{s}$ in excess of 2.1 to 2.2 GeV, and this leads to a fast improvement of agreement between data on pp and $\bar{p}p$ interactions. Thus, a detailed analysis of the results for $R_{\text{el/tot}}$ in nucleon–nucleon collisions at low energies confirms the qualitative conclusion drawn above that $R_{\text{el/tot}}(s)$ behaves similarly in elastic pp and $\bar{p}p$ reactions nearly over the whole energy region where one can compare experimental data on these two strong-interaction processes.

There are the following qualitative relationships between the approximating curves for the different parametrizations in Eq. (2) and different values of $s_{\min}$. In the case of the function in Eq. (2a), the fitted curves behave similarly at all of the $s_{\min}$ values being considered for any s reached in accelerator experiments. Moreover, this statement is also valid for the parametrization in Eq. (2b), in contrast to what we have in the case of individual samples for pp and $\bar{p}p$ interactions. For nucleon–nucleon collisions, the situation around the effect of the parametrization type at a fixed value of $s_{\min}$ is more ambiguous than that for pp and $\bar{p}p$ interactions. At the values of $\sqrt{s_{\min}} =$ 3 and 5 GeV, sizable distinctions between the two curves corresponding to expressions (2a) and (2b) are observed in the energy region of $\sqrt{s} \geq 10$ TeV, the distinction being much greater in the first case. But for the smallest value of the lower boundary of the fitting interval in energy, $\sqrt{s_{\min}} = 2$ GeV, the approximating curves obtained on the basis of the different functions in Eqs. (2) are very close to each other up to $\sqrt{s} \approx 100$ TeV, showing a sizable distinction only in the region of $\sqrt{s} \gtrsim 0.5$ PeV.

It is important to note that the hypothesis of the s independence of a phenomenological parameter associated with $R_{\text{el/tot}}(s)$ at intermediate energies in elastic pp and $\bar{p}p$ collisions [13] was considered before the appearance of the results from the LHC. Indeed, Figs. 1–3 show that the experimental dependence $R_{\text{el/tot}}(s)$ is nearly flat over a rather broad energy range from $\sqrt{s} \sim 5{-}10$ GeV to $\sqrt{s} \approx 63$ GeV. In order to obtain more comprehensive information, the ratio in (1) was approximated by a constant in the

Table 3. Fitted values of the parameters in $R_{\mathrm{el/tot}}(s)$ for a combined data sample for elastic pp and $\bar{p}p$ collisions

$\sqrt{s_{\min}}$, GeV	Parameter					
	a_1	$a_2 \times 10^3$	a_3	a_4	a_5	χ^2/NDF
			(2a)			
2	$(2.0 \pm 0.6) \times 10^{-4}$	7.8 ± 0.4	0.931 ± 0.017	0.638 ± 0.005	1.073 ± 0.013	3279/180
3	0.018 ± 0.006	9.9 ± 1.5	0.83 ± 0.06	0.64 ± 0.05	1.22 ± 0.12	230/88
5	0.153 ± 0.004	0.067 ± 0.028	2.30 ± 0.13	0.55 ± 0.17	1.92 ± 0.24	108/62
			(2b)			
2	0.155 ± 0.003	0.28 ± 0.11	1.80 ± 0.12	0.952 ± 0.026	0.822 ± 0.021	3191/180
3	0.169 ± 0.003	0.018 ± 0.003	2.7 ± 0.3	0.97 ± 0.18	0.91 ± 0.08	230/88
5	0.121 ± 0.006	1.0 ± 0.3	1.48 ± 0.11	0.207 ± 0.025	0.32 ± 0.04	105/62
			constant			
10^3	0.252 ± 0.003	–	–	–	–	9.72/9

intermediate-energy range of $s_1 \leq s \leq 10^4$ GeV^2. The results were the following: $a_0 = 0.1789 \pm 0.0008$ with $\chi^2/\mathrm{NDF} = 28.3/28$ at $\sqrt{s_1} = 10$ GeV for pp collisions; $a_0 = 0.1805 \pm 0.0017$ with $\chi^2/\mathrm{NDF} = 13.2/15$ at $\sqrt{s_1} = 5$ GeV for $\bar{p}p$ collisions; and $a_0 = 0.1786 \pm 0.0008$ with $\chi^2/\mathrm{NDF} = 33.4/37$ at $\sqrt{s_1} = 10$ GeV for nucleon–nucleon scattering. In the last case, the resulting approximation is represented by the thin line in Fig. 3, and the fitted values confirm the hypothesis of the s-independent behavior of $R_{\mathrm{el/tot}}(s)$ in either case of the individual samples for pp and $\bar{p}p$ interactions and in the case of a combined data set for nucleon–nucleon scattering at intermediate energies in the range being considered. However, measurements in the TeV-energy region indicate unambiguously that the hypothesis of constant $R_{\mathrm{el/tot}}(s)$ is valid only in some bounded energy range, and this effect is due to (i) a broad and flat minimum in $\sigma_{\mathrm{tot}}(s)$ and a nearly s-independent behavior of $\sigma_{\mathrm{el}}(s)$ in the intermediate-energy range of $5 \lesssim \sqrt{s} \lesssim 100$ GeV and/or (ii) a relatively small number of experimental points in the region of $\sqrt{s} > 0.5$ TeV for pp and $\bar{p}p$ collisions. Figure 3 confirms unambiguously these conclusions, demonstrating a smooth increase in $R_{\mathrm{el/tot}}(s)$ at energies in the region of $\sqrt{s} \gtrsim 5$ GeV. Therefore, the explicit effect of the invariability of $R_{\mathrm{el/tot}}(s)$ is most likely explained by kinematical (bounded range of s and large gap between two subsets of experimental data) and/or methodological (small volume of the data subset used) reasons rather than by dynamical features of strong-interaction processes. The growth of $R_{\mathrm{el/tot}}(s)$ is known to be a strong argument against the geometric model and can be viewed as a manifestation of the enhancement of (anti)nucleon opaqueness with increasing s [13].

3. SEARCHES FOR THE ONSET OF THE ASYMPTOTIC REGION

The analytic functions in Eqs. (2) and the fitted parameter values in Tables 1 and 2 permit evaluating the ratio $R_{\mathrm{el/tot}}$ at various collision energies. The estimates given below were obtained on the basis of the Standard Model (SM) without invoking any hypothesis concerning contributions from physics beyond it. It is well known that no evidence of the presence of physical processes and/or a particle beyond the SM that could affect the energy dependence of the parameters from the set $\mathcal{G}_{pp,\bar{p}p}$ has been obtained to date. Thus, the use of the SM-based approach seems justified. It should be noted that a continuous growth of the functions in Eqs. (2) with increasing s in the region of $\sqrt{s} \geq 3$ GeV is associated with the trend observed in available experimental data. It is natural to expect that a further increase in the collision energy s would lead to a saturation of $R_{\mathrm{el/tot}}(s)$ near the onset of the asymptotic regime. Obviously, this qualitative effect cannot be taken into account in a model-independent approximation. As was indicated above, the absence of experimental data for $\bar{p}p$ collisions in the region of multi-TeV energies leads to a substantial uncertainty in the behavior of $R_{\mathrm{el/tot}}(s)$ at high energies. Moreover, the majority of currently operating accelerator facilities (RHIC, LHC) and the international projects for a possible future hadron collider rated to higher energies (Future Circular Collider—FCC-hh; Super pp Collider—SPPC; and Very Large

Table 4. Estimates of $R_{\rm el/tot}(s)$ for pp interactions on the basis of fitted results at $\sqrt{s_{\rm min}} = 5$ GeV

Functions	$\sqrt{s}$, TeV							
	RHIC			LHC		HE-LHC, LHC limit		
	0.20	0.41	0.51	0.90	14	28	33	42
(2a)	0.19 ± 0.05	0.20 ± 0.06	0.20 ± 0.06	0.21 ± 0.07	0.27 ± 0.11	0.29 ± 0.12	0.29 ± 0.12	0.30 ± 0.12
(2b)	0.188 ± 0.023	0.20 ± 0.03	0.20 ± 0.03	0.21 ± 0.04	0.27 ± 0.09	0.29 ± 0.11	0.29 ± 0.11	0.30 ± 0.12
	SPPC, FCC-hh, VLHC-I, II							
	40	50	70.6	100	125	150	175	200
(2a)	0.30 ± 0.12	0.30 ± 0.13	0.31 ± 0.13	0.32 ± 0.14	0.33 ± 0.14	0.33 ± 0.15	0.34 ± 0.15	0.34 ± 0.15
(2б)	0.30 ± 0.12	0.31 ± 0.12	0.32 ± 0.14	0.33 ± 0.14	0.34 ± 0.15	0.34 ± 0.16	0.35 ± 0.16	0.35 ± 0.17
	Ultrahigh-energy cosmic rays					Energies in the PeV region		
	110	170	250	500	750	10^3	5×10^3	10^4
(2a)	0.33 ± 0.14	0.34 ± 0.15	0.35 ± 0.15	0.37 ± 0.17	0.38 ± 0.17	0.39 ± 0.18	0.43 ± 0.21	0.46 ± 0.22
(2б)	0.33 ± 0.15	0.35 ± 0.16	0.36 ± 0.17	0.39 ± 0.20	0.40 ± 0.21	0.41 ± 0.22	0.49 ± 0.29	0.5 ± 0.3

Hadron Collider—VLHC) rely on proton beams [14–16]. Therefore, the discussion given below is focused on pp scattering. Estimations for the energy ranges in the projects Facility for Antiproton and Ion Research (FAIR) and Nuclotron-based Ion Collider fAcility (NICA) are not performed for the reasons discussed in detail in [4].

A comparison of the different fitted curves shows that the weakest dependence of the results on the approximating-function type under the condition that the respective values of χ^2/NDF are statistically acceptable is observed at $\sqrt{s_{\rm min}} = 5$ GeV. For this reason, the estimates obtained for $R_{\rm el/tot}(s)$ on the basis of the results deduced by approximating the experimental data sample used for pp scattering by the functions in Eqs. (2a) and (2b) at $\sqrt{s_{\rm min}} = 5$ GeV (Table 1) are given in Table 4. As might have been expected, the values of $R_{\rm el/tot}(s)$ for the two functions being considered agree within the errors at any s. The ratio in (1) reaches the asymptotic level in the region of $\sqrt{s} \gtrsim 5$–10 PeV within 1.3 to 1.5 standard deviations for the function in Eq. (2a) and within larger uncertainties for the function in Eq. (2b), but the median values of $R_{\rm el/tot}(s)$ are still substantially smaller than 3/4 for either of the two functions in Eqs. (2). Thus, the results in Table 4 can be viewed only as an indication of the onset of the asymptotic regime in elastic pp collisions at $\sqrt{s_{\rm a}} \sim 5$–10 PeV. It is noteworthy that available experimental data permit obtaining a rather rough order-of-magnitude estimate for the boundary of the asymptotic energy region. From this point of view, the present estimate of $s_{\rm a}$ agrees quantitatively with the results obtained for the lower boundary of the asymptotic region in s for the cross sections $\sigma_{\rm tot}$, $\sigma_{\rm el}$, and $\sigma_{\rm inel}$ in the approach of partonic disks [17]. Moreover, the value obtained here for $s_{\rm a}$ is in reasonable agreement, at least at a qualitative level, with the results of the analysis performed in [18] in order to study the asymptotic behavior of $\sigma_{\rm tot}$ within the AQFT approach, but it is substantially smaller than the estimate that can be obtained for $s_{\rm a}$ with the aid of the parameter κ on the basis of the Regge–eikonal model [3]. Thus, we see that, by and large, the numerical results of the present study confirm unambiguously the important conclusion drawn on the basis of the other aforementioned approaches that the onset of the asymptotic region for global scattering parameters lies at energies in excess of at least $\mathcal{O}(100$ TeV) and, what is more probable, is in the region of multi-PeV energies. New experimental data of high statistical significance at energies of $\sqrt{s} \sim \mathcal{O}(100$ TeV), as well as the development of phenomenological models, are of paramount importance for refining estimates available for $s_{\rm a}$. Such data can be obtained in future collider experiments and in studies of ultrahigh-energy cosmic rays. Possibly, the choice of appropriate parameters that are sensitive to a transition to the asymptotic regime and a subsequent simultaneous phenomenological analysis of their s dependences would make it possible to improve the accuracy of quantitative estimates for the lower boundary of the asymptotic region in hadron collisions.

CONCLUSIONS

Summarizing the foregoing, we can draw the following conclusions.

A detailed analysis of the collision-energy dependence of the ratio of the elastic-to-total cross sections, $R_{\mathrm{el/tot}}$, has been performed for individual samples of pp and $\bar{p}p$ collision events, as well as for a combined sample of these interactions. Analytic approximations involving a generalized logarithmic term, which describes the region of high energies, and two different functional representations of the low-energy term have been proposed in order to approximate $R_{\mathrm{el/tot}}(s)$. These functions provide a reasonable description of all available experimental data everywhere for pp and $\bar{p}p$ collisions, with the exception of a narrow interval, $\sqrt{s} < 2$ GeV, near the lower boundary in energy for the latter case. The parametrizations in question provide statistically acceptable fits of similar quality over a broad energy region of $\sqrt{s} \geq 3$ GeV for pp and $\bar{p}p$ scattering. By and large, similar statements are also valid for a combined sample of nucleon–nucleon data, but the fit quality proves to be statistically acceptable at a somewhat larger value of the lower boundary of the fitting range, $\sqrt{s_{\min}} = 5$ GeV. Nevertheless, the proposed functions show reasonable agreement with qualitative trends observed in the combined data sample. This is so at almost all of the experimentally accessible energies in the region of $\sqrt{s} > 2$ GeV. Thus, we see that, in relation to other models, the parametrizations being considered provide a substantial extension of the described range toward the region of low energies. The dependence $R_{\mathrm{el/tot}}(s)$ admits an approximation by a constant within individual intervals at intermediate and high energies for all of the data samples being considered—that is, for pp, $\bar{p}p$, and nucleon–nucleon scattering—but this behavior of $R_{\mathrm{el/tot}}(s)$ is likely due to the boundedness of the fitting range and/or an insignificant number of experimental points in it rather than to some dynamical features of strong-interaction processes. Estimates for $R_{\mathrm{el/tot}}$ in elastic pp scattering at various values of s up to $\sqrt{s} = 10$ PeV have been obtained on the basis of the aforementioned approximations. These estimates show that the parameter being considered reaches its asymptotic value within 1.0 to 1.5 standard deviations in the energy region of $\sqrt{s} \gtrsim 5$–10 PeV, a specific result being dependent on the approximating-function type. However, significant uncertainties in the estimates at ultrahigh energies permit discussing the onset of the asymptotic regime for the parameter $R_{\mathrm{el/tot}}$ in elastic pp scattering only at a qualitative level. With allowance for the last statement, values in the range of $\sqrt{s_{\mathrm{a}}} \sim 5$–10 PeV can therefore be viewed only as a rough estimate for the lower boundary of the asymptotic region of energies. Anyway, the results of the present study confirm the important conclusion that the asymptotic region for hadron interactions lies far from the energies reached both in collider experiments and in cosmic-ray measurements.

ACKNOWLEDGMENTS

I am grateful to Professor V.A. Petrov for stimulating discussions.

This work was supported in part within the Program for Improving the Competitive Ability of National Research Nuclear University MEPhI (Contract no. 02.a03.21.0005 of August 27, 2013).

REFERENCES

1. I. M. Dremin, Phys. Usp. **61**, 381 (2018); Universe **04**, 65 (2018).
2. V. A. Okorokov and E. V. Sandrakova, Univ. J. Phys. Appl. **1**, 196 (2013); V. A. Okorokov, Int. J. Mod. Phys. E **22**, 1350041 (2013).
3. V. A. Petrov and V. A. Okorokov, Int. J. Mod. Phys. A **33**, 1850077 (2018).
4. V. A. Okorokov and S. D. Campos, Int. J. Mod. Phys. A **32**, 1750175 (2017).
5. Particle Data Group (C. Patrignani et al.), Chin. Phys. C **40**, 100001 (2016).
6. S. D. Campos and V. A. Okorokov, Int. J. Mod. Phys. A **25**, 5333 (2010).
7. V. A. Okorokov, Adv. High Energy Phys. **2015**, 914170 (2015); A data sample for the diffraction-cone slope is given in arXiv: 1501.01142 [hep-ph].
8. A. Martin, Phys. Rev. D **80**, 065013 (2009).
9. N. N. Bogolyubov, A. A. Logunov, A. P. Oksak, and I. T. Todorov, *General Principles of Quantum Field Theory* (Fizmatlit, Moscow, 2005; Springer, Netherlands, 1990).
10. V. A. Zorich, *Mathematical Analysis I* (MTsNMO, Moscow, 2002; Springer, Berlin, Heidelberg, 2004).
11. V. A. Okorokov, arXiv: 1805.10514 [hep-ph].
12. TOTEM Collab. (G. Antchev et al.), arXiv: 1712.06153 [hep-ex].
13. V. Barone and E. Predazzi, *High-Energy Particle Diffraction* (Springer, Berlin, Heidelberg, 2002).
14. M. Schaumann, Phys. Rev. Accel. Beams **18**, 091002 (2015).
15. J. Tang, J. Scott Berg, W. Chai, F. Chen, N. Chen, W. Chou, H. Dong, J. Gao, T. Han, Y. Leng, G. Li, R. Gupta, P. Li, Z. Li, B. Liu, Y. Liu, et al., arXiv: 1507.03224 [hep-ex].
16. The VLHC Design Study Group (G. Ambrosio et al.), Preprint Fermilab-TM-2149 (2001).
17. V. V. Anisovich, Phys. Usp. **185**, 963 (2015).
18. V. A. Okorokov, Phys. At. Nucl. **81**, 508 (2018).